nature immunology

Autonomous membrane IgE signaling prevents IgE-memory formation

Kei Haniuda, Saori Fukao, Tadahiro Kodama, Hitoshi Hasegawa & Daisuke Kitamura

Aberrant production of IgE antibodies can lead to allergic diseases. Normally, IgE$^+$ B cells rarely differentiate into memory B cells (B_{mem}) or long-lived plasma cells (LLPCs), as they only transiently participate in the germinal center (GC), but the mechanism behind this remains elusive. We found that membrane IgE (mIgE) autonomously triggered rapid plasma-cell differentiation and apoptosis independently of antigen or cellular context, predominantly through the mutually independent CD19-PI3K-Akt-IRF4 and BLNK-Jnk/p38 pathways, respectively, and we identified the ectodomains of mIgE as being responsible. Accordingly, deregulated GC IgE$^+$ B cell proliferation and prolonged IgE production with exaggerated anaphylaxis were observed in CD19- and BLNK-deficient mice. Our findings reveal an autonomous mIgE signaling mechanism that normally prevents IgE$^+$ B_{mem} and LLPC formation, providing insights into the molecular pathogenesis of allergic diseases.

IgE antibodies (Abs) are important for immunity against parasites and environmental substances such as venoms, but are best known as the mediator of type I hypersensitivity, which is the cause of various allergic diseases including asthma and anaphylaxis[1]. The half-life of IgE in serum is less than a few days, but IgE typically remains abnormally high for months or years in patients suffering from these diseases. In contrast, serum IgE Abs are normally almost undetectable in healthy individuals, even after recovery from infectious diseases, suggesting that there is active suppression of IgE production.

In typical T-cell-dependent (TD) immune responses that generate IgG or IgA Abs, antigen (Ag)-specific B cells are activated by cognate helper T cells, undergo class-switching, and then differentiate into short-lived plasma cells (SLPCs) or germinal center (GC) B cells. The GC B cells undergo somatic hypermutation (SHM) and affinity-based selection, and differentiate into memory B cells (B_{mem}) or long-lived plasma cells (LLPCs), both of which shape humoral memory. Although it is well established that B cells produce IgE as well as IgG1 Abs through class-switching in response to interleukin 4 (IL-4)[2], neither IgE$^+$ B_{mem} nor IgE$^+$ LLPCs appear to be generated, and serum IgE Abs do not accumulate, during normal TD responses. Several mechanisms for the negative regulation of IgE production have been suggested—for example, a low incidence of IgE class-switching[2] or negative feedback through the low-affinity IgE receptor CD23 (ref. 3)—but it is unclear whether these can account for the restricted formation of IgE$^+$ B_{mem} and LLPCs (IgE memory).

Owing to their rarity and resemblance to cells bearing IgE Ab bound via Fcε receptors, bona fide IgE$^+$ B cells have been difficult to detect *in vivo*, and their differentiation program has therefore long been enigmatic. IgE$^+$ B cells are mostly found outside GCs in peripheral lymphoid organs, express a plasma cell (PC) genetic program and have undergone SHM[4]. Three independent IgE-reporter mice lines revealed that IgE$^+$ B cells only transiently participate in the GC reaction and swiftly exit the GCs[5–8] before differentiating into B_{mem} or LLPCs. A number of mechanisms have been proposed for this. First, IgE$^+$ B cells express Blimp1, a master regulator of PC differentiation, and then differentiate into SLPCs[4,5]. Second, IgE$^+$ B cells are prone to apoptosis[5,6,9]. However, it is unknown why these events happen selectively in IgE$^+$ B cells.

Class-switched B cell receptors (BCRs), especially of membrane IgG (mIgG) and mIgE, have long cytoplasmic tails containing a highly conserved motif, which are responsible for provoking strong Ca^{2+} mobilization following BCR stimulation and for recall antibody responses[10–12]. Several signaling proteins binding to the cytoplasmic tail of mIgE have been identified[13,14], although none of them are specific to mIgE or have been found to be involved in the unique regulation of IgE$^+$ B cells. We hypothesized that mIgE itself harbors unique features that trigger the peculiar differentiation program of IgE$^+$ B cells independently of cell context. Our results reveal unique autonomous signaling by mIgE that is mediated by distinct molecular pathways that induces spontaneous PC differentiation and apoptosis of IgE$^+$ B cells, and thereby prevents IgE-memory formation.

RESULTS

Autonomous mIgE signaling induces differentiation to SLPC

Evidence showing the unique properties of class-switched B cells and BCRs[10,15] suggests that the mIgE-BCR itself affects IgE$^+$ B cell fate. To analyze the isotype-specific functions of BCR, we developed a culture system in which B cells express only a particular BCR of choice. We took splenic B cells from B1-8f C_γ1-Cre mice carrying both knock-in *Igh* alleles, one of which contained *loxP*-flanked *B1-8* V_H (ref. 16) and the other of which contained *C_γ1-Cre*[17], and cultured them with IL-4

Division of Molecular Biology, Research Institute for Biomedical Sciences, Tokyo University of Science, Noda, Japan. Correspondence should be addressed to D.K. (kitamura@rs.noda.tus.ac.jp).

Received 11 January; accepted 2 June; published online 18 July 2016; doi:10.1038/ni.3508

on feeder cells expressing CD40L and B cell activation factor (BAFF) (40LB), which facilitates proliferation of GC-like B cells (termed iGB cells) and class-switching to IgG1 or IgE[18] (**Fig. 1a**). As the B cells grew, more than 90% of the cells completely lost BCR expression by day 3 (**Supplementary Fig. 1a**). We then introduced NP-specific immunoglobulin heavy chain genes into these cells, resulting in a robust expression of BCR of each isotype (**Supplementary Fig. 1b**). This system, termed class-swapping, allowed us to analyze and directly compare the functions of each mIg isotype in the same context of primary cultured B cells.

To facilitate spontaneous differentiation to PC, we cultured the iGB cells without feeder cells and cytokines for a final day and then examined them for CD138 and Pax5 expression. Among the transduced isotypes, only mIgE induced significant differentiation to $CD138^+Pax5^{lo}$ PCs, although mIgA did so moderately (**Fig. 1b**), and apoptosis (**Fig. 1c**). Accordingly, mIgE upregulated the expression of *Irf4* and *Blimp1*, PC signature molecules, while suppressing *Bach2* and *Pax5* in sorted non-PC ($CD138^-$) iGB cells (**Fig. 1d**). Notably, stimulation of any of the BCR isotypes, except for mIgE, with anti-κ Ab more or less facilitated PC differentiation (**Supplementary Fig. 1c**), emphasizing the Ag-independent autonomous activation of mIgE signaling. These data suggest that the rapid differentiation of IgE^+ B cells to SLPCs[5] is primarily a result of cell-surface mIgE expression and does not require Ag engagement.

BCR stimulation activates downstream signaling cascades, including the MAP-kinase pathway, and upregulates IRF4 expression to promote PC generation[19]. We next transduced iGB cells with mIgE or mIgG1 to examine the activation of the BCR signaling cascades. Compared with mIgG1, which induced moderate changes only of the Erk kinase, mIgE induced phosphorylation of Src family kinases (SFKs), Syk, BLNK and MAP kinases (Erk, p38, Jnk), and expression of IRF4 (**Fig. 1e–g**). Moreover, as compared with mIgG1, mIgE elevated the basal intracellular calcium concentration ($[Ca^{2+}]_i$) without BCR stimulation (**Supplementary Fig. 1d–g**). mIgE also induced greater phosphorylation of the BCR co-receptor CD19 and the PI3K p85 subunit than mIgG1 (**Fig. 1h**). In addition, mIgE was abundantly co-precipitated with CD19, whereas mIgM and mIgG1 were only marginally so (**Fig. 1i**). The association of mIgE with CD19 was confirmed in non-lymphoid cells transduced with BCR and Igα/β, with or without CD19 (**Supplementary Fig. 1h** and data not shown), suggesting that no B-cell-specific components other than the BCR complex are needed for this association. Taken together, our results indicate that mIgE autonomously induces BCR downstream signaling and recruits CD19 to activate its downstream signaling, and alters the expression

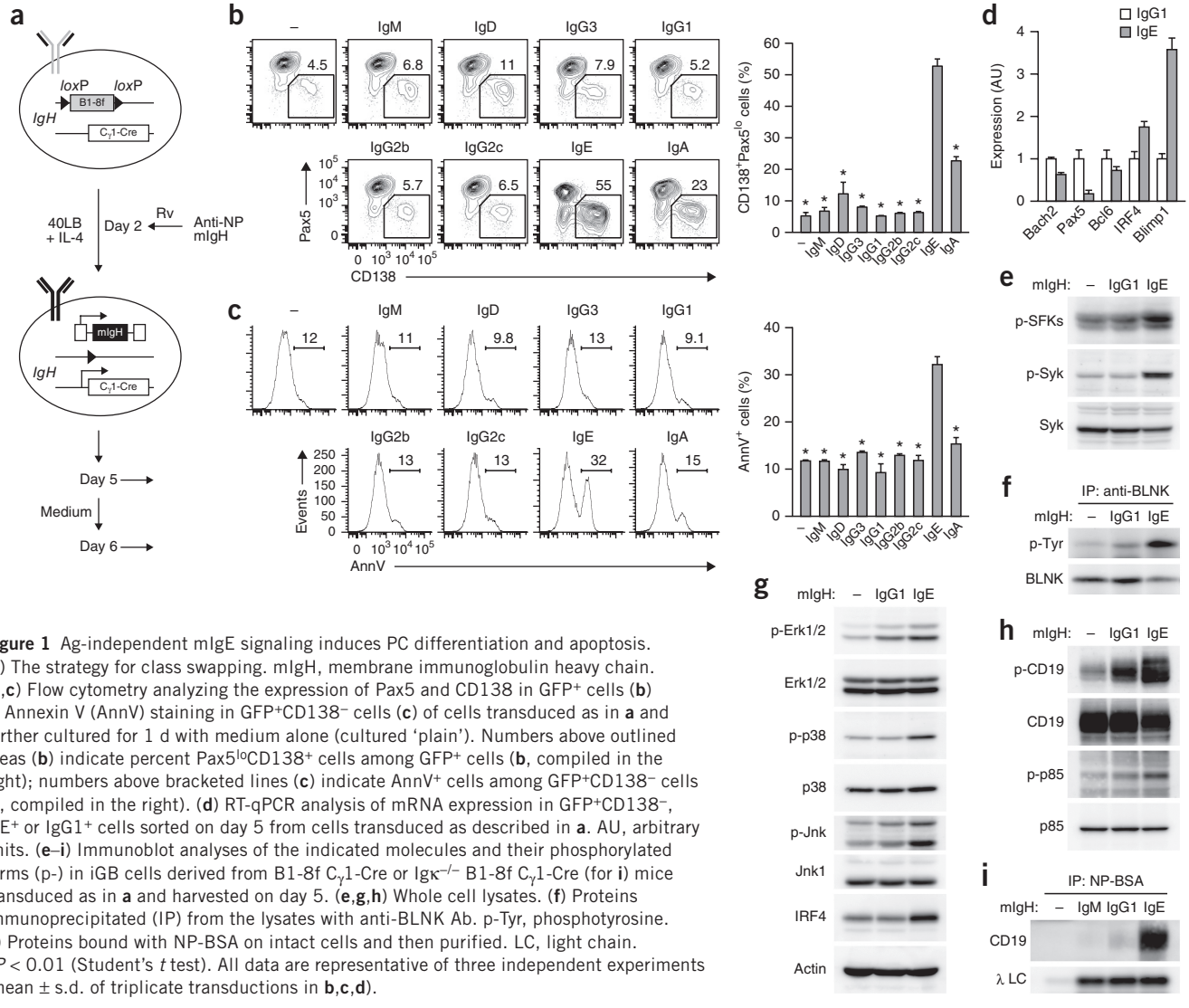

Figure 1 Ag-independent mIgE signaling induces PC differentiation and apoptosis. (**a**) The strategy for class swapping. mIgH, membrane immunoglobulin heavy chain. (**b**,**c**) Flow cytometry analyzing the expression of Pax5 and CD138 in GFP^+ cells (**b**) or Annexin V (AnnV) staining in GFP^+CD138^- cells (**c**) of cells transduced as in **a** and further cultured for 1 d with medium alone (cultured 'plain'). Numbers above outlined areas (**b**) indicate percent $Pax5^{lo}CD138^+$ cells among GFP^+ cells (**b**, compiled in the right); numbers above bracketed lines (**c**) indicate $AnnV^+$ cells among GFP^+CD138^- cells (**c**, compiled in the right). (**d**) RT-qPCR analysis of mRNA expression in GFP^+CD138^-, IgE^+ or $IgG1^+$ cells sorted on day 5 from cells transduced as described in **a**. AU, arbitrary units. (**e**–**i**) Immunoblot analyses of the indicated molecules and their phosphorylated forms (p-) in iGB cells derived from B1-8f $C_\gamma1$-Cre or $Ig\kappa^{-/-}$ B1-8f $C_\gamma1$-Cre (for **i**) mice transduced as in **a** and harvested on day 5. (**e**,**g**,**h**) Whole cell lysates. (**f**) Proteins immunoprecipitated (IP) from the lysates with anti-BLNK Ab. p-Tyr, phosphotyrosine. (**i**) Proteins bound with NP-BSA on intact cells and then purified. LC, light chain. $^*P < 0.01$ (Student's *t* test). All data are representative of three independent experiments (mean ± s.d. of triplicate transductions in **b**,**c**,**d**).

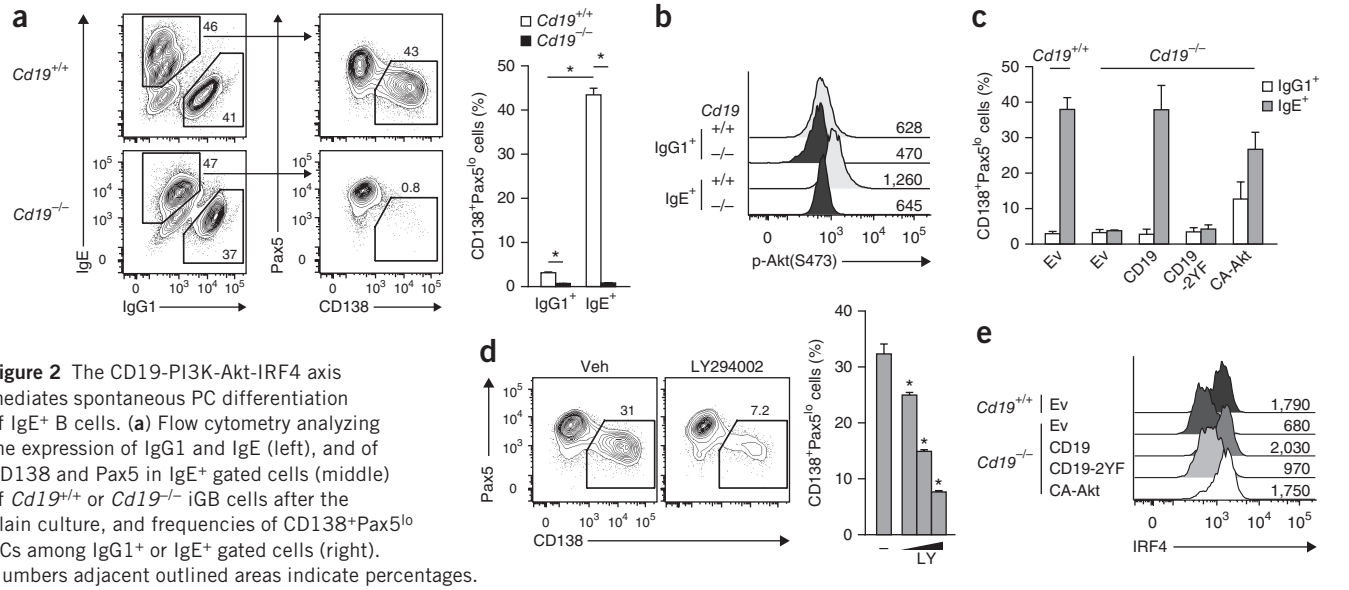

Figure 2 The CD19-PI3K-Akt-IRF4 axis mediates spontaneous PC differentiation of IgE$^+$ B cells. (**a**) Flow cytometry analyzing the expression of IgG1 and IgE (left), and of CD138 and Pax5 in IgE$^+$ gated cells (middle) of *Cd19*$^{+/+}$ or *Cd19*$^{-/-}$ iGB cells after the plain culture, and frequencies of CD138$^+$Pax5^{lo} PCs among IgG1$^+$ or IgE$^+$ gated cells (right). Numbers adjacent outlined areas indicate percentages. (**b**) Intracellular staining of p-Akt(S473) in gated CD138$^-$, IgG1$^+$ or IgE$^+$ cells on day 4 of the same cultures as in **a**. Numbers indicate geometric mean fluorescence intensity (geoMFI). (**c**) Frequencies of PCs among GFP$^+$, IgG1$^+$ or IgE$^+$ cells of *Cd19*$^{+/+}$ or *Cd19*$^{-/-}$ iGB cells transduced with empty Rv (IRES-GFP; Ev) or Rv with CD19, CD19-2YF,or CA-Akt, and cultured plain. (**d**) Flow cytometry of IgE$^+$ C57BL/6 iGB cells after the plain culture with LY294002 (LY: 0.63, 2.5, 10 μM) or vehicle only (Veh, –) for 1 d, and frequencies of PCs among the IgE$^+$ iGB cells (right). Numbers above outlined areas indicate percent PCs in a representative data of cells treated with 10 μM LY or Veh (left). (**e**) IRF4 expression in GFP$^+$IgE$^+$CD138$^-$ gated cells prepared as in **c** analyzed on day 5. Numbers indicate geoMFI. *$P < 0.01$ (Student's *t* test). Data are representative of three (**a**,**b**,**d**, mean and s.d. of triplicate culture in **a**,**d**) or two (**c**,**e**, mean and s.d. of two independent experiment in **c**) independent experiments.

of transcription factors associated with mature B cell differentiation, thereby promoting PC differentiation associated with apoptosis.

mIgE-induced PC differentiation needs a CD19-signaling axis

Given the robust CD19 recruitment and activation by mIgE, we examined the role of CD19 in mIgE-induced PC differentiation and apoptosis using B cells from CD19-deficient mice. The iGB cultures of *Cd19*$^{-/-}$ B cells had almost normal growth, with slightly less proliferation (**Supplementary Fig. 2a**), and slightly increased switching to IgE (**Supplementary Fig. 2b**). However, PC differentiation of *Cd19*$^{-/-}$ IgE$^+$ iGB cells was abrogated (**Fig. 2a**), even after BCR stimulation (**Supplementary Fig. 2c**). In contrast, mIgE-mediated apoptosis was not abrogated, but augmented (**Supplementary Fig. 2d**). Thus, CD19 appears to be necessary for PC differentiation, but not for apoptosis induction by mIgE expression. CD19 is known to signal through the PI3K-Akt pathway. Indeed, activation of the serine-threonine kinase Akt in IgE$^+$ iGB cells was attenuated by the lack of CD19 (**Fig. 2b**). Introduction of CD19 into *Cd19*$^{-/-}$ cells restored spontaneous PC differentiation of IgE$^+$ cells, whereas a CD19 mutant lacking PI3K binding motifs (2YF) did not. Constitutively active Akt

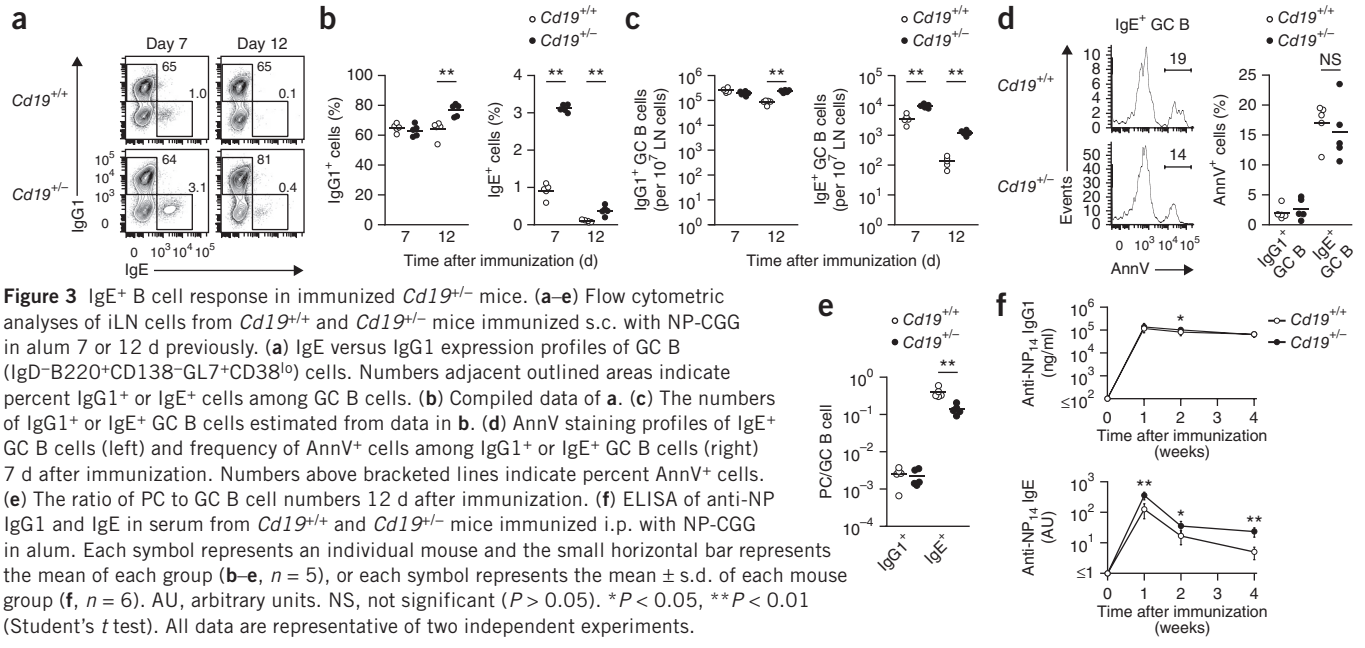

Figure 3 IgE$^+$ B cell response in immunized *Cd19*$^{+/-}$ mice. (**a**–**e**) Flow cytometric analyses of iLN cells from *Cd19*$^{+/+}$ and *Cd19*$^{+/-}$ mice immunized s.c. with NP-CGG in alum 7 or 12 d previously. (**a**) IgE versus IgG1 expression profiles of GC B (IgD$^-$B220$^+$CD138$^-$GL7$^+$CD38^{lo}) cells. Numbers adjacent outlined areas indicate percent IgG1$^+$ or IgE$^+$ cells among GC B cells. (**b**) Compiled data of **a**. (**c**) The numbers of IgG1$^+$ or IgE$^+$ GC B cells estimated from data in **b**. (**d**) AnnV staining profiles of IgE$^+$ GC B cells (left) and frequency of AnnV$^+$ cells among IgG1$^+$ or IgE$^+$ GC B cells (right) 7 d after immunization. Numbers above bracketed lines indicate percent AnnV$^+$ cells. (**e**) The ratio of PC to GC B cell numbers 12 d after immunization. (**f**) ELISA of anti-NP IgG1 and IgE in serum from *Cd19*$^{+/+}$ and *Cd19*$^{+/-}$ mice immunized i.p. with NP-CGG in alum. Each symbol represents an individual mouse and the small horizontal bar represents the mean of each group (**b**–**e**, $n = 5$), or each symbol represents the mean ± s.d. of each mouse group (**f**, $n = 6$). AU, arbitrary units. NS, not significant ($P > 0.05$). *$P < 0.05$, **$P < 0.01$ (Student's *t* test). All data are representative of two independent experiments.

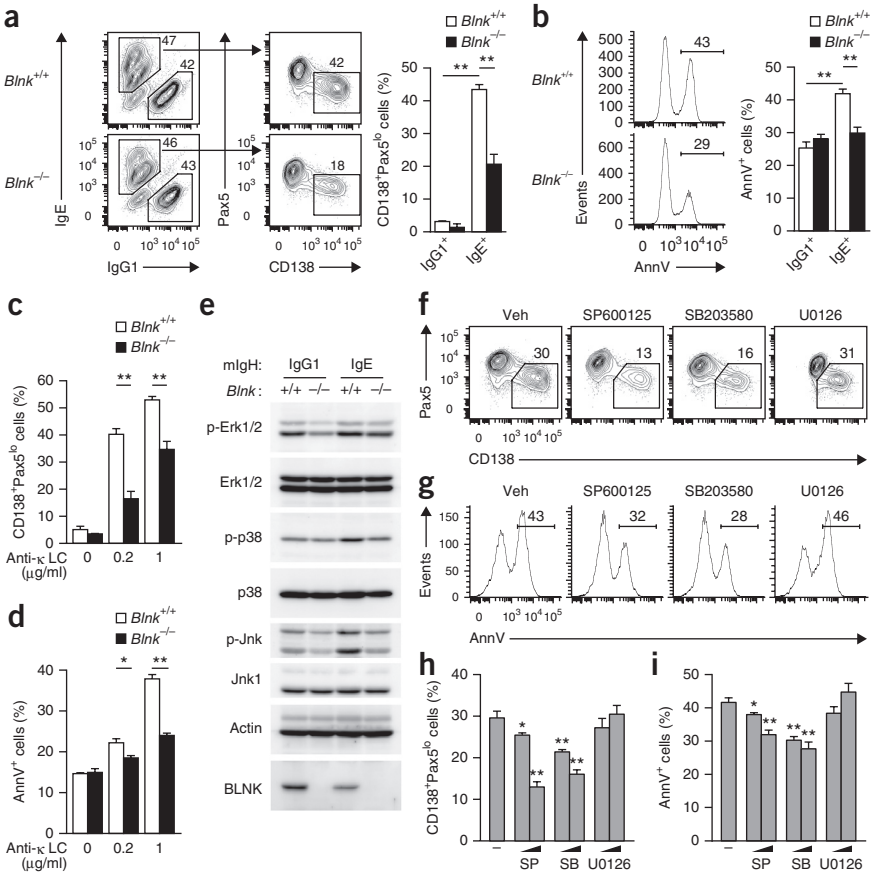

Figure 4 BLNK facilitates both PC differentiation and apoptosis of IgE$^+$ B cells. (**a**,**b**) Flow cytometric analyses of *Blnk*$^{+/+}$ or *Blnk*$^{-/-}$ iGB cells after the plain culture. (**a**) Expression profiles of IgG1 versus IgE (left) and CD138 versus Pax5 in IgE$^+$ gated cells (middle), with numbers adjacent outline areas indicating percentages, and frequencies of PCs among IgG1$^+$ or IgE$^+$ gated cells (right). (**b**) AnnV staining profiles of IgE$^+$CD138$^-$ cells, with numbers above bracketed lines indicating percent AnnV$^+$ cells (left), and frequencies of AnnV$^+$ cells among IgG1$^+$ or IgE$^+$, CD138$^-$ cells (right). (**c**,**d**) Flow cytometric analyses of *Blnk*$^{+/+}$ or *Blnk*$^{-/-}$ iGB cells after the plain culture with anti-κ LC Ab for 1 d. (**c**) Frequencies of PCs among IgG1$^+$ cells. (**d**) Frequencies of AnnV$^+$ cells among IgG1$^+$CD138$^-$ cells. (**e**) Immunoblot analyses of the indicated molecules in *Blnk*$^{+/+}$ or *Blnk*$^{-/-}$ B1-8f C_γ1-Cre iGB cells transduced with mIgG1 or mIgE as in **Figure 1a**. (**f**–**i**) Flow cytometric analyses of frequencies of PCs in IgE$^+$ cells (**f**,**h**) and AnnV$^+$ cells in IgE$^+$CD138$^-$ cells (**g**,**i**) of C57BL/6 iGB cells after plain culture with the addition of SP600125 (SP), SB203580 (SB), U0126 or vehicle only (Veh, –) for 1 d. Each inhibitor was added at 2.5 or 10 μM, with the latter used for the experiment shown as representative expression profiles (**f**,**g**). $^*P < 0.05$, $^{**}P < 0.01$ (Student's *t* test). Data are representative of three (**a**,**b**,**e**) or two (**c**,**d**,**f**–**i**) independent experiments (mean and s.d. of triplicate culture in **a**–**d**,**h**,**i**).

(CA-Akt) induced PC differentiation of IgE$^+$ *Cd19*$^{-/-}$ iGB cells and, to a lesser extent, of IgG1$^+$ *Cd19*$^{-/-}$ iGB cells (**Fig. 2c**). In addition, treatment with a PI3K inhibitor attenuated spontaneous PC differentiation of the IgE$^+$ *Cd19*$^{+/+}$ cells in a dose-dependent manner (**Fig. 2d**). IRF4 was more highly expressed in IgE$^+$ than in IgG1$^+$ CD138$^-$ iGB cells (**Supplementary Fig. 2e**). As expected, given the importance of IRF4 in PC generation[20], forced expression of IRF4 in iGB cells facilitated PC differentiation, but not apoptosis, of IgG1$^+$ and IgE$^+$ cells (**Supplementary Fig. 2f** and data not shown). Conversely, shRNA-mediated knockdown of IRF4 attenuated spontaneous PC differentiation of IgE$^+$ iGB cells (**Supplementary Fig. 2g**,**h**). The expression of IRF4 protein was lower in *Cd19*$^{-/-}$ than in *Cd19*$^{+/+}$ IgE$^+$ iGB cells, and it was restored by transduction of CD19 and CA-Akt, but not by CD19 2YF (**Fig. 2e**). Taken together, these data indicate that mIgE-associated CD19 induces the spontaneous PC differentiation program via PI3K-Akt-IRF4 signaling.

CD19 restrains IgE$^+$ GC B cell formation and IgE production

Next, we sought to clarify the function of CD19 in IgE$^+$ B cells *in vivo*. Given that *Cd19*$^{-/-}$ mice hardly produce any GCs or B cell memory[21] (data not shown), we decided to compare *Cd19*$^{+/-}$ and *Cd19*$^{+/+}$ mice. *In vitro* iGB culture revealed that *Cd19*$^{+/-}$ IgE$^+$ cells differentiated less well into PCs than *Cd19*$^{+/+}$ IgE$^+$ cells, whereas the extent of apoptosis was similar in both B cell genotypes; thus, we conclude that *Cd19*$^{+/-}$ IgE$^+$ cells had a milder *in vitro* phenotype than *Cd19*$^{-/-}$ IgE$^+$ B cells (**Supplementary Fig. 3a**,**b**). We immunized *Cd19*$^{+/-}$ and *Cd19*$^{+/+}$ mice with the TD Ag NP-CGG in alum and analyzed cells of the draining lymph nodes (LNs) by flow cytometry (**Supplementary Fig. 3c**). This analysis revealed that *Cd19*$^{+/-}$ mice had a higher frequency and number of IgE$^+$ GC B cells than *Cd19*$^{+/+}$ mice 7 and 12 d after immunization (**Fig. 3a**–**c**). Although the frequency of apoptotic IgE$^+$ GC B cells was equivalent between *Cd19*$^{+/-}$ and *Cd19*$^{+/+}$ mice (**Fig. 3d**), the PC-to-GC B-cell ratio in IgE$^+$ cells was significantly lower in *Cd19*$^{+/-}$ mice, indicating attenuated PC differentiation of *Cd19*$^{+/-}$ GC B cells (**Fig. 3e**). However, the serum anti-NP IgE titer was higher in *Cd19*$^{+/-}$ mice, suggesting more robust generation of IgE-producing LLPCs (**Fig. 3f**). The long-lasting higher concentration of serum IgE in *Cd19*$^{+/-}$ mice was pathologically manifested by an exaggerated systemic anaphylaxis response triggered at 10 weeks after primary immunization (**Supplementary Fig. 3d**). These data suggest that CD19 contributes to the early contraction of IgE$^+$ GC B cells by facilitating their differentiation to SLPCs, as well as to prevention of IgE$^+$ LLPC generation.

BLNK mediates mIgE-signaled PC differentiation and apoptosis

Given that phosphorylation of Syk, a pivotal BCR signal transducer, was enhanced by mIgE expression (**Fig. 1e**), we next assessed its role in the IgE$^+$ B cell fate decision. A Syk inhibitor blocked PC differentiation of IgE$^+$ iGB cells in a dose-dependent manner and substantially attenuated apoptosis (**Supplementary Fig. 4a**,**b**). Restoration of apoptosis at the highest doses of inhibitor may reflect Syk-mediated pro-survival BCR signaling[22]. Thus, Syk seems to be necessary for both PC differentiation and apoptosis signaled by mIgE expression.

We next examined the involvement of BLNK, an adaptor and a major Syk substrate, whose phosphorylation was markedly enhanced by mIgE expression (**Fig. 1f**). Proliferation and class-switching efficiency of *Blnk*$^{-/-}$ and *Blnk*$^{+/+}$ iGB cells were almost the same (**Supplementary Fig. 2a**,**b**), but spontaneous PC differentiation of *Blnk*$^{-/-}$ IgE$^+$ cells was attenuated and apoptosis induction was as low as in IgG1$^+$ cells (**Fig. 4a**,**b**). Essentially, the same result was

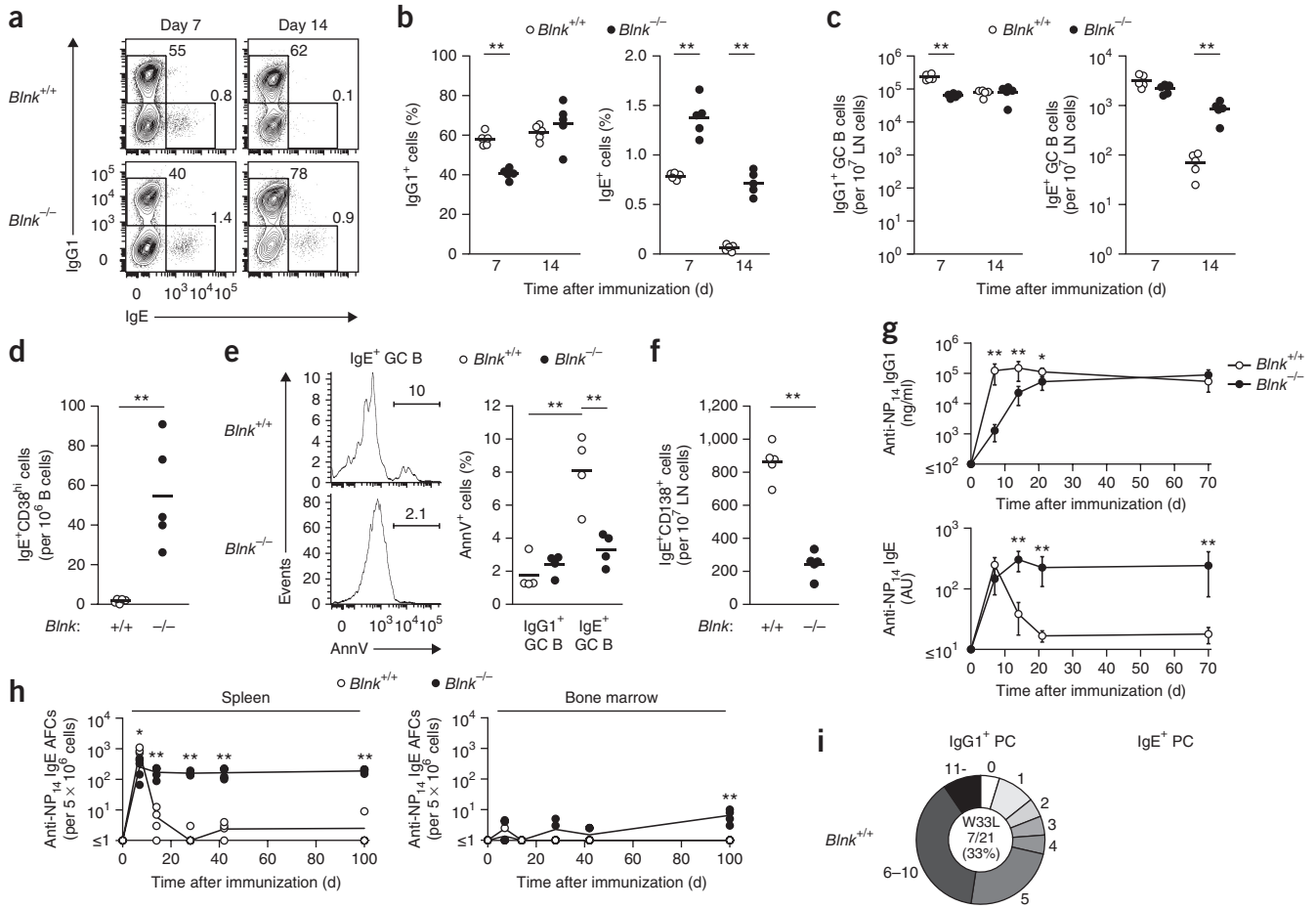

Figure 5 IgE+ B cell response in immunized BLNK-deficient mice. (**a**–**f**) Flow cytometric analyses of iLN cells from *Blnk*$^{+/+}$ and *Blnk*$^{-/-}$ mice immunized s.c. with NP-CGG in alum 7 or 14 d previously. IgE versus IgG1 expression profiles of GC B cells (**a**), frequencies (**b**) and the numbers (**c**) of IgG1+ and IgE+ GC B cells are analyzed as in **Figure 3a**. (**d**) The numbers of IgE+ B_{mem} cells (IgD−B220+CD138−GL7−CD38^{hi}) at day 14. (**e**) AnnV staining profiles of IgE+ GC B cells (left), and frequency of AnnV+ cells among IgG1+ or IgE+ GC B cells (right) at day 7. (**f**) The numbers of PCs at day 7. (**g**,**h**) ELISA of NP-specific IgG1 and IgE in serum (**g**) and ELISPOT assay of NP-specific IgE AFCs (**h**) from mice immunized i.p. with NP-CGG in alum. (**i**) SHM in NP-specific IgG1+ or IgE+ PCs from mice immunized as in **g** 4 weeks previously. Pie charts indicate frequency of V_H186.2 sequences with mutation numbers surrounding, and the ratio and frequencies (%) of the sequence with W33L replacement (center). Each symbol represents an individual mouse and small horizontal bar the mean of each group (**b**–**d**,**f**, $n = 5$; **e**,**h**, $n = 4$) or each symbol represents mean ± s.d. of each mouse group (**g**, $n = 6$). $^*P < 0.05$, $^{**}P < 0.01$ (Student's t test). Data are representative of three (**a**–**c**,**d**,**f**) or two (**e**,**g**,**h**) independent experiments, or pooled from three independent experiments with 7–10 mice for each genotype (**i**).

obtained in the class-swapping experiment using B cells from *Blnk*$^{-/-}$ and *Blnk*$^{+/+}$ mice crossed with B1-8f C_γ1-Cre mice (**Supplementary Fig. 4c**–**g**). BCR-stimulation-induced PC differentiation and apoptosis of IgG1+ iGB cells were also attenuated in the absence of BLNK (**Fig. 4c**,**d**). These results indicate that BLNK is involved in PC differentiation and, even more so, in the apoptosis induced by mIgE expression, perhaps through its spontaneous autoactivation.

BLNK is required for BCR-mediated calcium flux, as well as for activation of Jnk and p38 (ref. 23). Accordingly, mIgE-induced elevation of basal $[Ca^{2+}]_i$ was completely abrogated in BLNK-deficient iGB cells (**Supplementary Fig. 1d**–**g**). mIgE-induced hyperphosphorylation of p38 and Jnk was also abolished in the absence of BLNK in the class-swapping experiment, although Erk phosphorylation remained unchanged (**Fig. 4e**). Moreover, inhibition of Jnk or p38 significantly suppressed both PC differentiation and apoptosis of IgE+ iGB cells, but an inhibitor of MEK1/2, the upstream kinases of Erk, suppressed neither (**Fig. 4f**–**i**). These data suggest that BLNK-mediated activation of Jnk and p38 contributes to PC differentiation and apoptosis promoted by autonomous mIgE signaling.

BLNK suppresses generation of IgE+ GC B cell, B_{mem} and LLPC

To address the role of BLNK in mIgE-regulated late B cell development *in vivo*, we analyzed *Blnk*$^{-/-}$ and *Blnk*$^{+/+}$ mice immunized subcutaneously (s.c.) with NP-CGG in alum. Although the total number of GC B cells 7 d after immunization was lower in *Blnk*$^{-/-}$ mice, the frequency of IgE+ GC B cells in draining LNs was significantly higher compared with *Blnk*$^{+/+}$ mice, whereas that of IgG1+ cells was lower. The difference was more obvious by day 14, when the number of IgE+ GC B cells in *Blnk*$^{-/-}$ mice was approximately tenfold higher than in *Blnk*$^{+/+}$ mice (**Fig. 5a**–**c**). Accordingly, a significant number of IgE+ B_{mem} was present in *Blnk*$^{-/-}$ mice on day 14, whereas there were essentially none in *Blnk*$^{+/+}$ mice

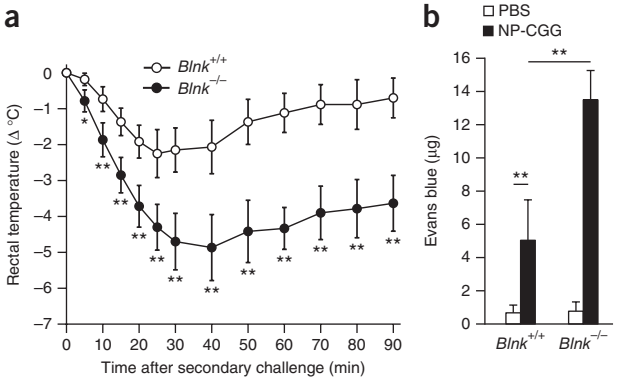

Figure 6 Enhanced active anaphylaxis in BLNK-deficient mice. Anaphylaxis reactions of *Blnk*$^{+/+}$ and *Blnk*$^{-/-}$ mice primed i.p. with NP-CGG in alum 100 d previously. (**a**) Changes in rectal temperature (Δ °C) of the mice injected intravenously (i.v.) with 5 μg NP-CGG (mean ± s.d., $n = 6$). (**b**) Measurement of extravasated dye in the ears of mice s.c. injected with 200 ng NP-CGG (right ears) and PBS (left ears) followed by i.v. injection with Evans blue dye, 30 min previously. Bar graphs represent the means with s.d. ($n = 7$, *Blnk*$^{+/+}$; $n = 6$, *Blnk*$^{-/-}$). $^{*}P < 0.05$, $^{**}P < 0.01$ (Student's *t* test). Data are representative of three (**a**) or two (**b**) independent experiments.

(**Fig. 5d**). By contrast, the frequency of apoptotic IgE^{+} GC B cells and the number of IgE^{+} PCs in *Blnk*$^{-/-}$ mice were markedly lower than those in *Blnk*$^{+/+}$ mice on day 7 (**Fig. 5e**,**f**). These data indicate that BLNK-mediated signaling promotes apoptosis and early PC differentiation of IgE^{+} GC B cells, and thereby inhibits their proliferation and subsequent development into B_{mem}.

Next, we accessed serum Ab levels over a long period after intraperitoneal (i.p.) immunization with NP-CGG in alum. The concentration of anti-NP IgG1 was initially very low in *Blnk*$^{-/-}$ mice, but reached normal amounts after 3 weeks (**Fig. 5g**). Anti-NP IgE peaked at 1 week in *Blnk*$^{+/+}$ mice and then rapidly declined, becoming almost undetectable by 3 weeks. In contrast, they remained high for at least 10 weeks in *Blnk*$^{-/-}$ mice (**Fig. 5g**). Accordingly, a significant number of anti-NP IgE Ab forming cells (AFCs) were maintained in the spleens of *Blnk*$^{-/-}$, but not of *Blnk*$^{+/+}$, mice (**Fig. 5h** and **Supplementary Fig. 5a**). In agreement with previous reports[5,24], only a few anti-NP IgE AFCs were observed in the bone marrow (**Fig. 5h** and **Supplementary Fig. 5a**). We sorted NP-specific IgE^{+} and IgG1^{+} single PCs from *Blnk*$^{-/-}$ and *Blnk*$^{+/+}$ mice 4 weeks after immunization (except for *Blnk*$^{+/+}$ IgE^{+} PCs, which were absent), and sequenced V_H186.2 genes that encode the anti-NP V_H regions in these cells (**Supplementary Fig. 5b**). Most *Blnk*$^{-/-}$ IgE^{+} PCs had mutated V_H regions and 42% of them had the W33L replacement mutation, an indication of anti-NP Ab affinity maturation, the levels of which were equivalent to those of *Blnk*$^{-/-}$ and *Blnk*$^{+/+}$ IgG1^{+} PCs (**Fig. 5i**). These data indicate that the *Blnk*$^{-/-}$ IgE^{+} PCs are LLPCs, which are believed to be generated in GCs, where they undergo SHM and affinity-based selection[25]. Thus, these results demonstrate that the BLNK-mediated signal suppresses the generation of IgE^{+} LLPCs.

Similarly, IgE^{+} LLPCs were produced after immunization in mixed bone-marrow chimeric mice in which BLNK deficiency was restricted to B cells (**Supplementary Fig. 5c–e**) or mice to which mature follicular B cells from B1-8f *Blnk*$^{-/-}$ mice were transferred (**Supplementary Fig. 5f–h**). The latter result excludes a possible contribution of immature B cells, which have been shown to preferentially switch to IgE[26], to the observed phenotype of *Blnk*$^{-/-}$ mice whose peripheral lymphoid organs are dominated by immature B cells[27,28]. Thus, mature B cells are primarily responsible for the abnormal IgE^{+} LLPC production in *Blnk*$^{-/-}$ mice.

The pathological relevance of the long-lasting IgE response in *Blnk*$^{-/-}$ mice was tested in active systemic and cutaneous anaphylaxis. Following secondary challenge with small doses of NP-CGG at 14 weeks after primary immunization, an exaggerated drop in body temperature and increased extravasation in the ears were observed in *Blnk*$^{-/-}$ mice as compared with *Blnk*$^{+/+}$ mice (**Fig. 6a**,**b**). Thus, BLNK-mediated regulation of IgE^{+} GC B cells appears to be important for preventing prolonged IgE production and anaphylaxis.

Distinct mIgE domains control BLNK- and CD19-signaling axes

Previous reports showed that mIgE recruits several signaling molecules via its cytoplasmic tail[10,13,14]. To elucidate which domain of mIgE promotes spontaneous PC differentiation and apoptosis, we constructed a series of chimeric γ1-ε heavy chains with the same V_H domain, and expressed them in iGB cells (**Fig. 7a** and **Supplementary Fig. 6a**). BCR with chimeric heavy chains consisting of transmembrane (TM)-cytoplasmic regions of IgG1 and ectodomains of IgE (EctoE) induced spontaneous PC differentiation and apoptosis to the same extent as a complete mIgE, whereas that of IgE TM-cytoplasmic regions and IgG1 ectodomains (EctoG1) did not (**Fig. 7b–e**). Moreover, mIgE lacking almost all of the cytoplasmic tail (IgE ΔTail) induced PC differentiation and apoptosis, albeit to a somewhat reduced extent than complete mIgE (**Supplementary Fig. 6b–d**). These data indicate that the mIgE cytoplasmic tail has no specific role and that its ectodomains are primarily responsible for triggering autonomous signaling to induce PC differentiation and apoptosis.

Serial replacement of the ectodomains of IgG1 from N-terminal CH1 to CH3 with those of IgE from CH1 to CH4 revealed that the CH1-CH4 domains of IgE were not sufficient for the induction of PC differentiation; rather, additional replacement of the extracellular membrane-proximal domain (EMPD) from IgG1 to IgE was required (**Fig. 7b**,**c**). This observation correlated well with the association of each immunoglobulin molecule with CD19, as only mIgE and EctoE abundantly bound to (**Fig. 7f**) and induced phosphorylation of CD19 (**Fig. 7g**), suggesting that the EMPD of mIgE (εEMPD) is responsible for its interaction with CD19. To confirm this, we constructed a chimeric mIgG1 (EMPD-E) in which the EMPD was replaced with the εEMPD (**Supplementary Fig. 6e**,**f**). Expression of EMPD-E on iGB cells did not induce apoptosis and only marginally induced PC differentiation compared with the complete mIgE (**Supplementary Fig. 6g–j**). However, EMPD-E was abundantly co-precipitated with CD19 and induced more phosphorylation of CD19 than complete mIgG1 (**Supplementary Fig. 7a**,**b**). These data indicate that εEMPD is necessary and sufficient for the interaction with CD19, and is necessary, but not sufficient, for spontaneous PC differentiation.

In contrast, the CH1-4E induced apoptosis as strongly as EctoE and mIgE (**Fig. 7d**,**e**). The apoptosis induction capacity of the chimeric molecules largely correlated with their ability to phosphorylate Syk and BLNK (**Fig. 7d**,**e**,**h**,**i** and **Supplementary Fig. 7c**,**d**). In addition, mIgE-induced phosphorylation of CD19 was unaffected by the lack of BLNK, and the amount of BLNK phosphorylation in mIgE^{+} cells was not reduced in the absence of CD19 (**Supplementary Fig. 7e–g**), suggesting that BLNK and CD19 are activated independently of each other. Collectively these data indicate that the two main axes of autonomous mIgE signaling, mediated by BLNK and CD19, are triggered by distinct ectodomains of mIgE (**Supplementary Fig. 7h**).

DISCUSSION

IgE^{+} B cells are generated during immune responses, but are extremely short lived because they swiftly differentiate to SLPCs and then die

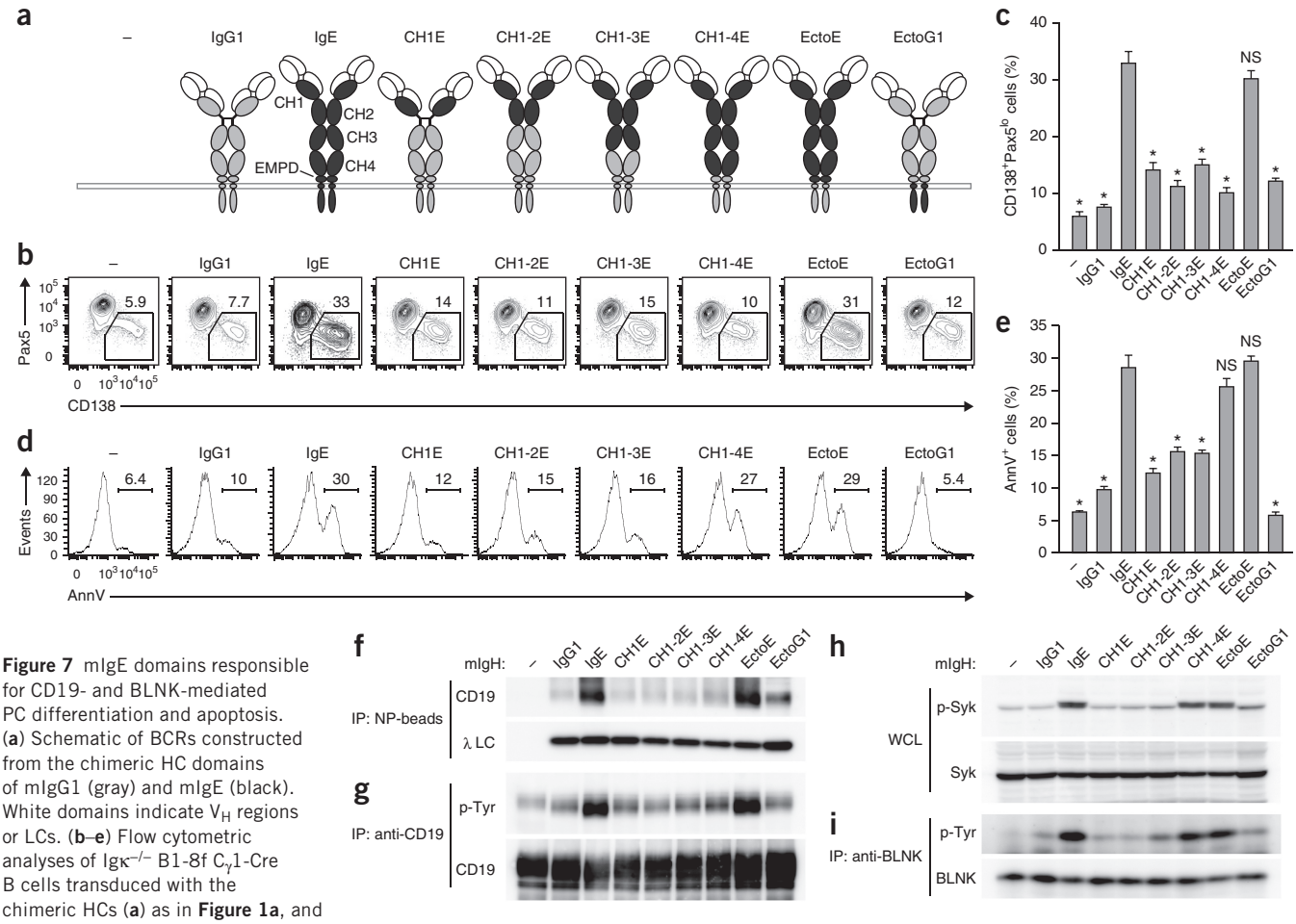

Figure 7 mIgE domains responsible for CD19- and BLNK-mediated PC differentiation and apoptosis. (**a**) Schematic of BCRs constructed from the chimeric HC domains of mIgG1 (gray) and mIgE (black). White domains indicate V_H regions or LCs. (**b**–**e**) Flow cytometric analyses of Igκ$^{-/-}$ B1-8f C_γ1-Cre B cells transduced with the chimeric HCs (**a**) as in **Figure 1a**, and cultured plain. CD138 versus Pax5 expression profiles, with numbers indicating percent PCs (**b**), AnnV staining profiles, with numbers indicating percent AnnV$^+$ cells (**d**), and frequencies of PCs among GFP$^+$ cells (**c**) and AnnV$^+$ cells among GFP$^+$CD138$^-$ cells (**e**). (**f**–**i**) Immunoblot analyses of the indicated molecules in the same cells as in **a**–**e** lysed on day 5. (**f**) Proteins purified by NP-beads incubated with the cell lysates. (**g**) Proteins immunoprecipitated (IP) from the lysates with anti-CD19 Ab. (**h**) Whole-cell lysates (WCLs). (**i**) Proteins immunoprecipitated from the lysates with anti-BLNK Ab. NS, not significant ($P > 0.05$); *$P < 0.01$ (Student's t test) as compared with IgE. Data are representative of three (**b**–**e**,**g**,**h**; mean and s.d. of triplicate transductions in **c**,**e**) or two (**f**,**i**) independent experiments.

by apoptosis[5,6,9]. We found that, among BCR classes, mIgE uniquely promoted immediate differentiation to PC and apoptosis in primary-cultured GC-like B (iGB) cells following surface expression and that this response was independent of Ag stimulation. This autonomous mIgE signaling was brought about by the extracellular region and not, as predicted, the cytoplasmic tail of mIgE, and activated and required two independent pathways mediated by CD19 and BLNK.

CD19 was essential for mIgE-driven PC differentiation of iGB cells, and the CD19-PI3K-Akt signaling axis leading to IRF4 upregulation promoted PC differentiation. IRF4 is indispensable for PC development and is thought to form a homodimer to activate the *Prdm1* locus encoding Blimp1 (refs. 19,20). On the other hand, BLNK only partially contributed to mIgE-driven PC differentiation. BLNK is not required for the mIgE-induced phosphorylation of CD19, and most likely mediates the PC differentiation through Jnk and/or p38 activation. Our results suggest that the CD19-PI3K-Akt-IRF4 axis is essential for PC differentiation downstream of autonomous mIgE signaling, whereas the BLNK-Jnk/p38 axis may have an enhancing role.

As for mIgE-promoted apoptosis, BLNK has an essential role, whereas CD19 is rather anti-apoptotic. We found that *in vivo*, in the absence of BLNK, the frequency of apoptotic IgE$^+$ B cells declined to a level equivalent to IgG1$^+$ B cells. Our *in vitro* data also suggests that BLNK-mediated Jnk/p38 activation promotes the apoptosis of IgE$^+$ B cells. A number of studies have proposed mechanisms of apoptosis induction by Jnk/p38—for example, phosphorylation-induced activation of the pro-apoptotic Bim and inactivation of the anti-apoptotic Bcl-2 proteins[29,30]—that might be relevant to mIgE-promoted apoptosis.

Using mIgG1-IgE chimeric molecules, we found that the ectodomains of mIgE are responsible for the characteristic IgE$^+$ B cell responses. Dissection of the ectodomains revealed that Cε1-Cε4 were responsible for autonomous Syk-BLNK phosphorylation and apoptosis induction, but were not sufficient for PC differentiation, which required the additional εEMPD, as did CD19 phosphorylation. In the context of mIgG1, the εEMPD alone was sufficient for the interaction with CD19 and its phosphorylation, but not for PC differentiation, suggesting that both Cε1-Cε4-mediated auto-signaling and the εEMPD-CD19 interaction are required for PC differentiation. IgE Ab has a unique bent structure[31] and has a high mannose-type N-linked glycan on the Cε3 domain that affects IgE structure[32], suggesting that the entire structure of the Cε1-Cε4 domains is critical for mIgE function. Indeed, replacement or deletion of any one of the Cε domains of mIgE attenuated PC differentiation and apoptosis induction (data

not shown). Taken together, we propose that Cε1-Cε4 ectodomains compose an inseparable structural unit that is responsible for autonomous signal transduction from mIgE, whereas εEMPD recruits CD19 and promotes activation of CD19-associated PI3K by Syk. Although currently unclear, the unique mIgE ectodomain structure may mediate reorganization of the BCR complexes such as by self-association or dissociation[33] and/or binding of unidentified molecule(s) to autonomously activate signaling.

Although autonomous mIgE signaling is a unique feature among BCR isotypes, its outcome is quite similar to antibody-stimulated signaling of mIgG1 on iGB cells, which also induces CD19- and BLNK-dependent PC differentiation and apoptosis. GC B cells mostly consisting of IgG^+ were reported to rapidly undergo apoptosis following stimulation with soluble cognate Ag *in vivo*, a scenario reflecting the physiological elimination of autoreactive B cells that arise in GCs as a result of SHM[34–36]. Although GC B cells are generally silent in BCR signaling as a result of high phosphatase activity, the cells in G_2/M phase of cell cycle residing mainly in the dark zone (DZ) are an exception[37,38] and therefore they may get triggered by auto-Ags. Similarly, apoptosis of IgE^+ GC B cells is presumed to occur in the DZ before migration to the light zone[6,39]. Thus, IgE^+ B cells are likely to be eliminated in GCs by apoptosis when mIgE signaling becomes autonomously activated after entering the G_2/M phase in the DZ.

Analyses of immune responses in BLNK- and CD19-deficient mice provided strong *in vivo* evidence indicating that autonomous mIgE signaling through BLNK and CD19 induces SLPC instead of GC-B/B_{mem}/LLPC fate for IgE^+ B cells. However, we and others[6] failed to demonstrate activation of mIgE signaling or elevated expression of PC signature molecules in *ex vivo* IgE^+ GC B cells. This is probably because mIgE auto-signaling can be activated only in a small fraction of them, namely those in the G_2/M phase of the cell cycle, as described above. In addition, the IgE^+ cells may rapidly lose GC B-cell markers once the PC program is initiated *in vivo*, making IgE^+ GC B cells even scarcer. iGB cells as a model of GC B cells were useful to overcome such quantitative problems. It has been reported that inducible expression of a constitutively active Syk in B cells induces Blimp1 expression and promotes SLPC differentiation and apoptosis[40], and that expression of LMP2A, which mimics strong tonic BCR-signaling in B cells, accelerates PC differentiation and reduces the number of GC B cells[41]. Thus, it is likely that, as we propose for autonomous mIgE signaling, activation of BCR signaling in a particular phase of GC B cells, rather than dampening of it[6], causes their differentiation into SLPCs and apoptosis, perhaps through Syk, BLNK and CD19.

In summary, we propose that remodeling of the BCR complexes through mIgE ectodomains autonomously activates their signal transduction, as represented by Syk activation, and downstream, mutually independent CD19-PI3K-Akt-IRF4 and BLNK-Jnk/p38 axes. This drives rapid PC differentiation and death of IgE^+ GC B cells, thereby preventing generation of IgE^+ B_{mem} and LLPCs. Thus, defects in either signaling axis can result in the formation of IgE^+ B_{mem} and LLPCs, followed by prolonged and recall IgE production, resulting in allergic disease. Although congenital defects of key BCR signaling molecules such as BLNK or CD19 cause early arrest of human B cell development[42], somatic loss or detrimental modification of such molecules in responding B cells may cause allergic diseases. Alternatively, congenital or somatic variations altering mIgE structure or mIgE-specific binding proteins may also be pathogenic. Thus, elucidation of such defects could lead to development of new strategies to prevent allergic disorders.

METHODS

Methods and any associated references are available in the online version of the paper.

Note: Any Supplementary Information and Source Data files are available in the online version of the paper.

ACKNOWLEDGMENTS

We thank K. Rajewsky and colleagues (Max Delbrück Center for Molecular Medicine) for B1-8f, C_γ1-Cre and *Cd19*$^{-/-}$ mice, F. Alt (Harvard Medical School) and T. Tsubata (Tokyo Medical and Dental University) for *Igκ*$^{-/-}$ mice, T. Azuma (Research Institute for Biomedical Sciences) for N1G9 cDNA, M. Ohkura and J. Nakai (Saitama University) for G-CaMP6, T. Kitamura (University of Tokyo) for pMXs-IRES-GFP and Plat-E cells, J. Yagi (Tokyo Women's Medical University School of Medicine) for CA-Akt, RIKEN BRC for Balb/c 3T3 cells, J. Nakayama, M. Yamamoto and S. Horiuchi for plasmid constructs, T. Nojima, R. Goitsuka, M. Kubo and other members of the Research Institute for Biomedical Sciences for technical advice and comments, and P. Burrows for critical reading. This work was supported by the Japan Society for the Promotion of Science (JSPS) KAKENHI (25293116 to D.K., 15K19138 and 12J08178 to K.H.) and Takeda Science Foundation (D.K.). K.H. was a JSPS Fellow when he started this study.

AUTHOR CONTRIBUTIONS

K.H. conceived the project, designed and performed all of the experiments, analyzed data, and wrote the manuscript. S.F. performed experiments, analyzed data, gave critical advice and edited the manuscript. T.K. and H.H. provided technical support. D.K. supervised the study, designed experiments and wrote the manuscript.

COMPETING FINANCIAL INTERESTS

The authors declare no competing financial interests.

1. Galli, S.J. & Tsai, M. IgE and mast cells in allergic disease. *Nat. Med.* **18**, 693–704 (2012).
2. Geha, R.S., Jabara, H.H. & Brodeur, S.R. The regulation of immunoglobulin E class-switch recombination. *Nat. Rev. Immunol.* **3**, 721–732 (2003).
3. Yu, P., Kosco-Vilbois, M., Richards, M., Köhler, G. & Lamers, M.C. Negative feedback regulation of IgE synthesis by murine CD23. *Nature* **369**, 753–756 (1994).
4. Erazo, A. *et al.* Unique maturation program of the IgE response in vivo. *Immunity* **26**, 191–203 (2007).
5. Yang, Z., Sullivan, B.M. & Allen, C.D. Fluorescent in vivo detection reveals that IgE^+ B cells are restrained by an intrinsic cell fate predisposition. *Immunity* **36**, 857–872 (2012).
6. He, J.-S. *et al.* The distinctive germinal center phase of IgE^+ B lymphocytes limits their contribution to the classical memory response. *J. Exp. Med.* **210**, 2755–2771 (2013).
7. Lafaille, J.J., Xiong, H. & Curotto de Lafaille, M.A. On the differentiation of mouse IgE^+ cells. *Nat. Immunol.* **13**, 623–624, author reply 623–624 (2012).
8. Talay, O. *et al.* IgE^+ memory B cells and plasma cells generated through a germinal-center pathway. *Nat. Immunol.* **13**, 396–404 (2012).
9. Laffleur, B. *et al.* Self-Restrained B Cells Arise following Membrane IgE Expression. *Cell Rep.* **10**, 900–909 (2015).
10. Engels, N. *et al.* Recruitment of the cytoplasmic adaptor Grb2 to surface IgG and IgE provides antigen receptor-intrinsic costimulation to class-switched B cells. *Nat. Immunol.* **10**, 1018–1025 (2009).
11. Achatz, G., Nitschke, L. & Lamers, M.C. Effect of transmembrane and cytoplasmic domains of IgE on the IgE response. *Science* **276**, 409–411 (1997).
12. Kaisho, T., Schwenk, F. & Rajewsky, K. The roles of gamma 1 heavy chain membrane expression and cytoplasmic tail in IgG1 responses. *Science* **276**, 412–415 (1997).
13. Oberndorfer, I. *et al.* HS1-associated protein X-1 interacts with membrane-bound IgE: impact on receptor-mediated internalization. *J. Immunol.* **177**, 1139–1145 (2006).
14. Geisberger, R. *et al.* Phage display based cloning of proteins interacting with the cytoplasmic tail of membrane immunoglobulins. *Dev. Immunol.* **9**, 127–134 (2002).
15. Wang, N.S. *et al.* Divergent transcriptional programming of class-specific B cell memory by T-bet and RORα. *Nat. Immunol.* **13**, 604–611 (2012).
16. Lam, K.P., Kühn, R. & Rajewsky, K. In vivo ablation of surface immunoglobulin on mature B cells by inducible gene targeting results in rapid cell death. *Cell* **90**, 1073–1083 (1997).

17. Casola, S. *et al.* Tracking germinal center B cells expressing germ-line immunoglobulin gamma1 transcripts by conditional gene targeting. *Proc. Natl. Acad. Sci. USA* **103**, 7396–7401 (2006).
18. Nojima, T. *et al.* In-vitro derived germinal centre B cells differentially generate memory B or plasma cells in vivo. *Nat. Commun.* **2**, 465 (2011).
19. Ochiai, K. *et al.* Transcriptional regulation of germinal center B and plasma cell fates by dynamical control of IRF4. *Immunity* **38**, 918–929 (2013).
20. Klein, U. *et al.* Transcription factor IRF4 controls plasma cell differentiation and class-switch recombination. *Nat. Immunol.* **7**, 773–782 (2006).
21. Rickert, R.C., Rajewsky, K. & Roes, J. Impairment of T-cell-dependent B-cell responses and B-1 cell development in CD19-deficient mice. *Nature* **376**, 352–355 (1995).
22. Hobeika, E. *et al.* CD19 and BAFF-R can signal to promote B-cell survival in the absence of Syk. *EMBO J.* **34**, 925–939 (2015).
23. Ishiai, M. *et al.* BLNK required for coupling Syk to PLC gamma 2 and Rac1-JNK in B cells. *Immunity* **10**, 117–125 (1999).
24. Achatz-Straussberger, G. *et al.* Migration of antibody secreting cells towards CXCL12 depends on the isotype that forms the BCR. *Eur. J. Immunol.* **38**, 3167–3177 (2008).
25. Tarlinton, D. B-cell memory: are subsets necessary? *Nat. Rev. Immunol.* **6**, 785–790 (2006).
26. Wesemann, D.R. *et al.* Immature B cells preferentially switch to IgE with increased direct Sμ to Sε recombination. *J. Exp. Med.* **208**, 2733–2746 (2011).
27. Jumaa, H. *et al.* Abnormal development and function of B lymphocytes in mice deficient for the signaling adaptor protein SLP-65. *Immunity* **11**, 547–554 (1999).
28. Hayashi, K. *et al.* The B cell-restricted adaptor BASH is required for normal development and antigen receptor-mediated activation of B cells. *Proc. Natl. Acad. Sci. USA* **97**, 2755–2760 (2000).
29. Cai, B., Chang, S.H., Becker, E.B., Bonni, A. & Xia, Z. p38 MAP kinase mediates apoptosis through phosphorylation of BimEL at Ser-65. *J. Biol. Chem.* **281**, 25215–25222 (2006).
30. Yamamoto, K., Ichijo, H. & Korsmeyer, S.J. BCL-2 is phosphorylated and inactivated by an ASK1/Jun N-terminal protein kinase pathway normally activated at G_2/M. *Mol. Cell. Biol.* **19**, 8469–8478 (1999).
31. Wan, T. *et al.* The crystal structure of IgE Fc reveals an asymmetrically bent conformation. *Nat. Immunol.* **3**, 681–686 (2002).
32. Shade, K.-T.C. *et al.* A single glycan on IgE is indispensable for initiation of anaphylaxis. *J. Exp. Med.* **212**, 457–467 (2015).
33. Yang, J. & Reth, M. The dissociation activation model of B cell antigen receptor triggering. *FEBS Lett.* **584**, 4872–4877 (2010).
34. Pulendran, B., Kannourakis, G., Nouri, S., Smith, K.G. & Nossal, G.J. Soluble antigen can cause enhanced apoptosis of germinal-centre B cells. *Nature* **375**, 331–334 (1995).
35. Shokat, K.M. & Goodnow, C.C. Antigen-induced B-cell death and elimination during germinal-centre immune responses. *Nature* **375**, 334–338 (1995).
36. Han, S., Zheng, B., Dal Porto, J. & Kelsoe, G. *In situ* studies of the primary immune response to (4-hydroxy-3-nitrophenyl)acetyl. IV. Affinity-dependent, antigen-driven B cell apoptosis in germinal centers as a mechanism for maintaining self-tolerance. *J. Exp. Med.* **182**, 1635–1644 (1995).
37. Khalil, A.M., Cambier, J.C. & Shlomchik, M.J. B cell receptor signal transduction in the GC is short-circuited by high phosphatase activity. *Science* **336**, 1178–1181 (2012).
38. Victora, G.D. *et al.* Germinal center dynamics revealed by multiphoton microscopy with a photoactivatable fluorescent reporter. *Cell* **143**, 592–605 (2010).
39. He, J.S. *et al.* Biology of IgE production: IgE cell differentiation and the memory of IgE responses. *Curr. Top. Microbiol. Immunol.* **388**, 1–19 (2015).
40. Hug, E., Hobeika, E., Reth, M. & Jumaa, H. Inducible expression of hyperactive Syk in B cells activates Blimp-1-dependent terminal differentiation. *Oncogene* **33**, 3730–3741 (2014).
41. Minamitani, T. *et al.* Evasion of affinity-based selection in germinal centers by Epstein-Barr virus LMP2A. *Proc. Natl. Acad. Sci. USA* **112**, 11612–11617 (2015).
42. Minegishi, Y. *et al.* An essential role for BLNK in human B cell development. *Science* **286**, 1954–1957 (1999).

ONLINE METHODS

Mice and immunizations. C57BL/6NCrSlc (B6) mice were purchased from Japan SLC. All the following mice were backcrossed to the B6 or B6-CD45.1 strain. B1-8f mice[16], C_γ1-Cre mice[17], *Igκ*$^{-/-}$ mice[43], *Cd19*$^{-/-}$[21] and *Blnk*$^{-/-}$ mice[44] were described previously. Mice were immunized i.p. with 100 μg of $NP_{32\text{-}36}$-CGG in alum except for flow cytometry of iLN cells, mice were immunized s.c. with 50 μg of NP-CGG in alum in both flanks and 25 μg in both sides of the tail base (150 μg/mouse). Sex-matched 6-14 week old mice were used for all experiments. Number of mice used for experiments is stated in figure legends. All mice were maintained in Tokyo University of Science (TUS) mouse facility under specific pathogen-free conditions. Mouse procedures were performed under protocols approved by the TUS Animal Care and Use Committee.

Plasmid constructions. For IgM, IgD, IgG3, IgG1, IgG2b, IgG2c and IgE, cDNA was prepared from B6 naive B or iGB cells, or GC B cells from B6 mice immunized with SRBC 12 days earlier, and for IgA, from B cells cultured 4 d in the presence of LPS (10 μg/ml, *Escherichia coli* 055:B5; Sigma), TGF-β1 (2 ng/ml; R&D Systems), IL-5 (5 ng/ml; Peprotech) and retinoic acid (10 nM; Sigma). From these cDNAs, C_H sequences of immunoglobulin heavy chains were amplified by using KOD Fx Neo or plus Neo DNA polymerases (Toyobo), and subcloned into pBluescript II SK (Invitrogen). IRF4, CD19, Igα and Igβ were also cloned from cDNA of B6 iGB cells. All chimeric immunoglobulins and the CD19 2YF mutant, in which two YxxM motifs (Y482 and Y513; PI3K-binding motif) were replaced with FxxM motifs, were generated by PCR-based mutagenesis. For Flag-tagged CD19 (BM40 signal peptide-Flag-CD19), BM40 signal peptide and Flag tag were added to the N-terminal of CD19 in place of the original signal peptide by PCR-based mutagenesis. Each C_H cDNA was ligated to a V gene sequence from NP-specific N1G9 hybridoma, and the resultant heavy chain cDNA was cloned into pMXs-IRES-GFP or pMXs-IRES-N1G9-λ1, in which a GFP sequence was replaced with a λ1 light chain cDNA of N1G9, or pMXs-IRES-mCherry, in which the GFP sequence was replaced with an mCherry sequence. IRF4, CD19, CD19 2YF and CA-Akt (E40K)[45] were cloned into pMXs-IRES-GFP. Igα and Igβ were cloned into pMX-IRES-hCD8 and pMX-IRES-rCD2[46], respectively. For RNAi, the following sequences were selected as the targets of shRNA: Luciferase, 5′-GTGCGTTGCTAGTACCAA-3′; IRF4-1, 5′-GCAATGACTTTGAGGAATTGG-3′; IRF4-2, 5′-GCTGCATAT CTGCCTGTATTA-3′, and inserted into pSIREN-hNGFR in which the puromycin resistance gene of pSIREN-RetroQ vector (Clontech) was replaced with a cytoplasmic-tail-truncated human NGFR cDNA (hNGFR). The calcium indicator G-CaMP6[47] was cloned into pMXs-IRES-hNGFR, in which the GFP sequence was replaced with the hNGFR sequence.

Flow cytometry. Single-cell suspensions prepared as described[46] were stained with Abs and reagents listed in **Supplementary Table 1** For IgE staining of iLN cells, intracellular staining was performed as described[5]. IgG1 staining of iLN cells, IgG1 and IgE staining of iGB cells were performed as total (surface and intracellular) staining using a Cytofix/Cytoperm solution and Perm/Wash buffer (BD Biosciences) according to the manufacturer's protocol. In **Supplementary Figure 1e**, IgG1 and IgE on the surface of live iGB cells were stained. IRF4 staining was performed using Foxp3 Staining Buffer Set (eBioscience). Pax5 and p-Akt staining was performed successively using Fixation Buffer (BD Biosciences) and Perm III buffer (BD Biosciences). Annexin V was stained using the Annexin V Apoptosis Detection Set (eBioscience) according to the manufacturer's instruction. All samples were analyzed using a FACSCallibur, FACSAria II or FACSCanto II (BD Biosciences). For analysis of G-CaMP fluorescence, iGB cells transduced with G-CaMP and mIgG1 or mIgE were stained with APC-conjugated anti-hNGFR antibody in RPMI-1640 medium containing 0.5% BSA. Cells were washed twice, resuspended in RPMI-1640 medium without phenol red containing 0.5% BSA, and analyzed by FACSCallibur. The data were analyzed using FlowJo (Tree Star).

Cell purification and culture. Naive B cell purification and iGB cell culture were performed as described[18]. B cells were cultured in 'B-cell medium' (RPMI-1640 medium (Wako) supplemented with 10% FCS, 10 mM HEPES, 1 mM sodium pyruvate, 5.5×10^{-5} M 2-ME, 100 U/ml penicillin, and 100 μg/ml streptomycin (GIBCO)). 40LB feeder cells were removed from the iGB cultures using anti-H2Kd (BioLegend) Ab, Streptavidin Particle Plus DM and an IMag system (BD Biosciences). iGB cells were harvested on day 4 of the culture. In the experiments to assess PC differentiation and apoptosis, isolated iGB cells on day 4 were further cultured for 1 d in B-cell medium alone without feeder cells and cytokines (plain culture).

Retroviral transduction. For production of retrovirus, pMXs vectors were transfected into Plat-E cells by Fugene HD (Promega) or PEI "Max" (Mw 40,000; Polysciences). The virus-containing supernatant was harvested 2 d after transfection and added to day 2 iGB cells, typically in triplicate. Cells were spin-infected at 2,000 rpm, 32 °C for 90 min with 10 μg/ml DOTAP Liposomal Transfection Reagent (Roche) and IL-4 (1 ng/ml; Peprotech). One day later, cells were harvested, replated on new 40LB feeder layers with IL-4, and harvested on day 5. For the class swapping procedure, B cells from B1-8f C_γ1-Cre mice were cultured on 40LB cells with IL-4 and transduced with each membrane immunoglobulin heavy chain (mIgH) or empty vector (–) as above. In the experiments to assess PC differentiation and apoptosis, iGB cells were isolated on day 5 and further cultured 'plain' as described above.

Preparation of 3T3 cells expressing Igα/β. pMX vectors encoding Igα and Igβ were transfected into Plat-E cells by Fugene HD (Promega). The virus-containing supernatant was harvested 2 d after transfection, and added to BALB/c 3T3 cells (clone A31, RIKEN BRC) in 6-well plates. Then cells were spin-infected at 2,000 rpm, 32 °C for 90 min with 10 μg/ml DOTAP Liposomal Transfection Reagent (Roche). 3 d after infection, hCD8 and rCD2 double positive single cells were directly sorted into 96-well plates using FACSAria II (BD Biosciences).

Quantitative RT-PCR. Total RNA was extracted, reverse-transcribed and subjected to quantitative PCR as described[18].

Immunoblotting and immunoprecipitation. Cells were lysed with 1% NP-40 lysis buffer containing protease- and phosphatase-inhibitors. Lysates were mixed with sample buffer, boiled and used for SDS-PAGE, followed by immunoblotting using Abs in **Supplementary Table 1**. For immunoprecipitation, precleared lysates were incubated with appropriate Abs and protein G- or streptavidin-conjugated Sepharose beads (GE Healthcare) at 4 °C with mild agitation. After extensive washing with 0.5% NP-40 buffer, the precipitates were boiled in sample buffer and subjected to SDS-PAGE, followed by immunoblotting. Two methods were used in this study to purify BCR complexes: For **Figure 1i**, cells were incubated in B-cell medium with 10 μg/ml biotinylated NP_{14}-BSA for 5 min on ice, washed twice with ice-cold PBS, lysed with 1% NP-40 lysis buffer, and then streptavidin-conjugated Sepharose beads (GE Healthcare) were added to the lysates. After 1 h incubation with mild agitation at 4 °C, the beads were washed extensively with 0.5% NP-40 buffer and then boiled in sample buffer. For **Figure 7f** and **Supplementary Figures 1f** and **7a**, harvested cells were lysed with 1% NP-40 lysis buffer, and NP-conjugated Sepharose beads (Biosearch Technologies) were added to the cell lysates. After 1 h incubation with mild agitation at 4 °C, the beads were washed extensively with 1% NP-40 lysis buffer and then boiled in sample buffer.

ELISA and ELISPOT assays. Serum titers of NP-specific IgG1 and IgE were analyzed by ELISA and NP-specific AFCs were detected by ELISPOT using NP_{14}-BSA as described[46]. Anti-NP IgE spots were revealed by biotinylated anti-mouse IgE Ab (R35-118; BD Biosciences) in conjunction with HRP conjugated streptavidin (Southern Biotech).

Active anaphylaxis. Mice were primed i.p. with 100 μg of NP-CGG in alum. For active systemic anaphylaxis, the primed mice were administrated 5 or 20 μg of soluble NP-CGG i.v. as a secondary immunization, and then rectal temperature was measured using a TD-300 (Shibaura electronics). For active cutaneous anaphylaxis, the primed mice were injected subcutaneously with 200 ng of soluble NP-CGG into the right ear and PBS into the left ear, followed by i.v. injection of 250 μl Evans blue dye (5 mg/ml; Wako). 30 min later, the ears were dissected and Evans blue dye was extracted in formamide at 60 °C for 16 h. Dye concentration was determined by OD 620 nm.

doi:10.1038/ni.3508

Plasma cell sorting and V_H sequence analysis. Plasma cells were magnetically enriched from pooled spleens and iLNs cells using anti-CD138 antibody and the MACS system (Miltenyi Biotec), then fixed and permeabilized with Cytofix/Cytoperm solution (BD Biosciences), and stained with anti-IgG1 and anti-IgE Abs and Alexa647-conjugated NP-BSA in Perm/Wash buffer (BD Biosciences). Then, NP-specific $IgG1^+$ or IgE^+ single plasma cells were directly sorted using FACSAria II (BD Biosciences), as shown in **Supplementary Figure 5b**, into 10 µl KOD Fx Neo buffer (Toyobo) containing 0.1 mg/ml proteinase K (Merck) in 96-well plates. The plates were incubated at 55 °C for 1 h followed by 95 °C for 10 min (heat-inactivation), and then 5 µl of a mixture of KOD Fx Neo buffer, dNTPs (Toyobo), primers and KOD DNA polymerase (Toyobo) were added per well. To amplify V_H186.2 sequences, the first round PCR was performed with 94 °C for 2 min, and then 35 cycles of 98 °C for 10 s, 55 °C for 30 s, 68 °C for 50 s. The second round was also performed using KOD Fx Neo with the following conditions: 94 °C for 2 min, and then 30 cycles of 98 °C for 10 s, 55 °C for 30 s, 68 °C for 50 s. Sequences of the primers used for the PCRs were the same as described previously[5]. PCR products were purified with ExoProStar (GE Healthcare) according to the manufacturer's instructions and sequenced (Eurofins Genomics).

Generation of bone marrow chimeric mice and adoptive transfer. Bone marrow cells from at least three mice of each indicated genotype were mixed at the indicated ratio, injected i.v. (5×10^6 cells per mouse) into lethally irradiated B6 mice (5.5 Gy, twice at 3-h intervals) as described previously[46]. 8 weeks after the transfer, the chimeric mice were used for immunization. For mature B cell transfer, $CD21^{med}CD23^{hi}CD24^{lo}B220^+$ mature follicular B cells were sorted from pooled spleens of mice (at least two) by using FACSAria II (BD Biosciences). This procedure yielded > 95% purity (Data not shown). 4×10^5 sorted cells were transferred into B6 mice and then the mice were immunized i.p. with 100 µg NP-CGG in alum 1 d after transfer.

Statistical analysis. Statistical analyses were performed by a two-tailed unpaired Student's *t* test.

43. Chen, J. *et al.* B cell development in mice that lack one or both immunoglobulin kappa light chain genes. *EMBO J.* **12**, 821–830 (1993).
44. Hayashi, K., Yamamoto, M., Nojima, T., Goitsuka, R. & Kitamura, D. Distinct signaling requirements for Dmu selection, IgH allelic exclusion, pre-B cell transition, and tumor suppression in B cell progenitors. *Immunity* **18**, 825–836 (2003).
45. Arimura, Y. *et al.* Akt is a neutral amplifier for Th cell differentiation. *J. Biol. Chem.* **279**, 11408–11416 (2004).
46. Fukao, S., Haniuda, K., Nojima, T., Takai, T. & Kitamura, D. gp49B-mediated negative regulation of antibody production by memory and marginal zone B cells. *J. Immunol.* **193**, 635–644 (2014).
47. Ohkura, M. *et al.* Genetically encoded green fluorescent $Ca2^+$ indicators with improved detectability for neuronal $Ca2^+$ signals. *PLoS One* **7**, e51286 (2012).